Growth of molybdenum and tungsten on GaAs in a molecular beam epitaxy system

J. Bloch,[a] M. Heiblum, and Y. Komem[b]
IBM Thomas J. Watson Research Center, Yorktown Heights, New York 10598

(Received 26 November 1984; accepted for publication 12 March 1985)

Thin films of Mo and W were grown on top of (100) GaAs in a molecular beam epitaxy system. Mo grew epitaxially between 200 and 450 °C with its (111) plane parallel to (100) GaAs plane. W grew as a random polycrystalline deposit. For both metals, interaction with the GaAs occurred during growth at 500 °C. Schottky barrier heights determined by current and capacitance measurements show that the electrical properties of the metal-GaAs interface do not strongly depend on the growth temperature and the microstructure of the films.

Metal-semiconductor junctions are of prime technological importance due to their vast number of applications, especially as Schottky barriers (detectors, field-effect transistor gates, hot-electron injectors)[1–3] and ohmic contacts.[4] The metal–*n*-GaAs interface attracts interest in particular, because of the poorly understood mechanism of the Schottky barrier formation[5] and the relatively unreliable ohmic contacts available.[4] The use of molecular beam epitaxy (MBE), which enables the growth of intimate clean junctions,[6] can significantly help in the study of such interfaces.

Among the many metals for which growth mechanisms on GaAs have been investigated,[7] Mo and W are believed not to react with GaAs upon heat treatment below ~600 °C and may be useful as diffusion barriers for Ga and As.[8,9] However, recent results suggest that an interface reaction occurs even at room temperature in a zone ~10 Å wide.[10] Both Mo and W have a bcc structure with similar lattice constants, namely, 3.15 Å for Mo and 3.16 Å for W. The interesting question is whether and how such a structure can grow epitaxially on GaAs that has a zincblende structure with a lattice constant of 5.654 Å. Iron is the only bcc metal that has been grown epitaxially on GaAs, and this is due to their good lattice match.[11]

We report here the growth of Mo and W on MBE grown (100) GaAs epilayers under UHV conditions. Special attention was devoted to material purity, interface cleanliness, and minimization of background impurities during evaporation. Electron diffraction patterns, Auger results, and Schottky barrier studies on the Mo-GaAs and W-GaAs systems will be presented.

Two 5-kW electrostatic electron gun evaporators[12,13] were built for the *in situ* evaporation of refractory metals. All parts that are subject to excess heat are made of electron-beam-melted Mo or Ta. Special precautions were taken to prevent the escape of elastically scattered electrons, which cause outgassing from the chamber walls.[14] The guns were mounted into a RIBER 1000-1 MBE system, below a LN_2 cooled shroud. With a system base pressure of 2×10^{-11} Torr prior to the evaporation, the pressure increased to 5×10^{-10} Torr during Mo, and 2×10^{-9} Torr during W evaporations (mostly due to hydrogen). The pressure measured by an ion gauge situated in the substrate position, due to the flux of metal atoms, was $\sim(5\text{–}10)\times10^{-9}$ Torr, for growth rates of 1–3 Å/min.

Conductive (100) oriented GaAs substrates were cleaned and mounted onto a Ta block using Ga. Following growth at 600 °C of ~1 μm GaAs doped with Si to $\sim1\times10^{17}$ cm^{-3},[15] the substrate temperature was reduced and held at T_s ~300 °C in the chamber, until background pressure reached $\sim5\times10^{-11}$ Torr. Thereafter, T_s was brought to the desired growth temperature, and metal evaporation was initiated. Growth rates of 1–3 Å/min, and typical layer thickness of 150 Å were used. Reflection high-energy electron diffraction patterns were monitored during growth, and Auger electron spectra were taken *in situ* immediately after the evaporation was completed. The samples were then removed and prepared for transmission electron microscopy studies and Schottky barrier height measurements.

Electron diffraction results reveal that the metal film structures are determined by substrate temperature for which there are three distinct regions. (1) At low temperatures, the films are polycrystalline and randomly oriented. (2) At an intermediate region of temperatures, preferred orientation and epitaxial growth are achieved. (3) At high temperatures, the metals react with GaAs. The tendency toward preferred orientation starts at $T_s = 100$ °C for Mo and 250 °C for W, and increases at higher temperatures.

The evolution of the RHEED patterns during the growth of Mo at substrate temperatures between 200 and 400 °C consists of the following steps. Initially, the surface reconstruction followed by the bulk features of the GaAs disappears completely after a coverage of approximately 5 Å. In the following 20–35-Å deposition, the screen shows a high background level without any defined pattern; thereafter, the Mo patterns appears abruptly. Presently we do not understand the reason for this phenomenon. The RHEED patterns of the Mo initially appear in the form of wide and elongated streaks, reconfirming that the surface is reasonably smooth but somewhat distorted [Fig. 1(a)]. As the deposition continues, the streaks change to round dots, as shown in Fig. 1(b), suggesting a three-dimensional structure. After deposition of ~50 Å, the film exhibits a steady-state structure that does not change significantly up to 150 Å. An interpretation of the RHEED patterns is possible only after the epitaxial relations are established from the TEM patterns, and will be discussed later.

[a] Nuclear Research Center, Negev, P. O. Box 9001, Beer Sheva, Israel.
[b] Department of Materials Engineering, Technion, Israel Institute of Technology, Haifa, Israel.

Downloaded 16 Aug 2008 to 132.77.4.43. Redistribution subject to AIP license or copyright; see http://apl.aip.org/apl/copyright.jsp

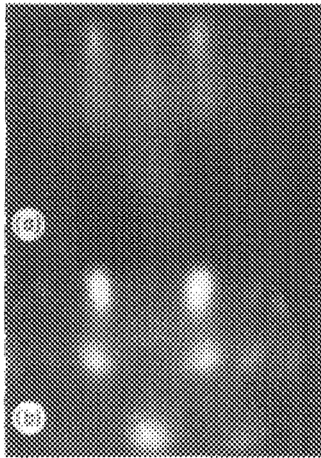

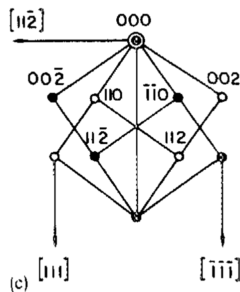

FIG. 1. RHEED patterns of Mo grown on (100) GaAs at 270 °C. (a) After a growth of ~50 Å; (b) after growth of ~150 Å; (c) interpretation of (b), with the parent domain orientation shown by (○) and the twinned one by (●). The 000 diffraction spot does not appear in the micrographs of (a) and (b).

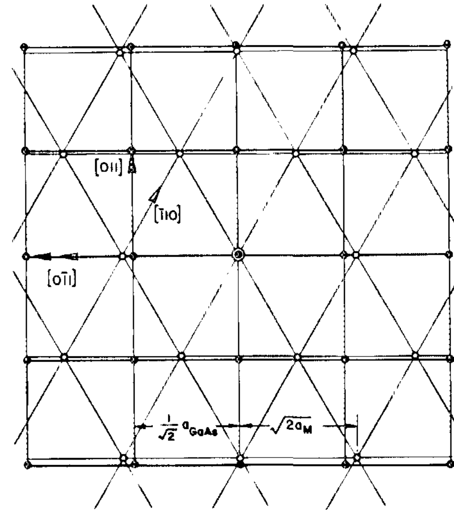

FIG. 2. Schematic atom arrangements of (111) Mo ‖ (100) GaAs, with [0$\bar{1}$1] Mo ‖ [0$\bar{1}$1] GaAs. (●) GaAs atoms. (○) metal atoms. Solid and open arrows show directions in the GaAs and the metal lattices, respectively.

The TEM results exhibit, as also observed in the RHEED patterns, that at a minimum growth temperature of 200 °C, the Mo films grow epitaxially. Figures 3 and 4 are the diffraction pattern and the bright-field image, respectively, for an electron beam perpendicular to the (100) surface of the GaAs. The epitaxial arrangement is (111) Mo ‖ (100) GaAs with the [0$\bar{1}$1] Mo ‖ [0$\bar{1}$1] GaAs, as proposed by the model in Fig. 2. Here the smallest nearest neighbor linear misfits are 11.5%, whereas the second neighbor misfits in the [011] GaAs direction are -3.5%. On top of a fixed (100) GaAs, the (111) Mo may assume four separate orientations, each rotated by 30° relative to the other. As shown by the electron image in Fig. 4, the film is composed of small crystallites, with an average size of several hundred angstroms. The Moiré patterns which characterize separate crystallites confirm the epitaxial orientation of each grain. X-ray diffraction of the same film reveals a (222) Mo peak, with a width that corresponds to an average crystallite size of 120 ± 20 Å. Crystallites having similar azimuthal orientations are grouped into domains; each domain is several thousands angstroms in size. In each domain the crystallites are oriented within a small angle relative to the [0$\bar{1}$1] of GaAs. This is shown in Fig. 4 by the misalignment between the Moiré patterns of different crystallites in the same domain and by the small arcing, spanning 2°–3°, of the Mo spots in the diffraction pattern of Fig. 3. The reason for this small-angle rotation is not clear, but it may be related to the large misfit between the two lattices.

A simple explanation of the RHEED pattern is now possible and is given in Fig. 1(c). This figure shows two domains: one with the orientation shown in Fig. 2 and another where the Mo is rotated by 30 °C. These domains are related through twining about the [11$\bar{2}$] direction, and Fig. 1(b) is a combined diffraction pattern for both. This RHEED pattern is taken along the [010] GaAs or [$\bar{1}$10] Mo and is repeated every 60° of azimuthal rotation.

The discussed epitaxial growth persists up to $T_s \sim 450$ °C. At 520 °C, a substantial chemical reaction between Mo and GaAs takes place, as indicated by changes in the diffraction patterns of the RHEED and TEM. The main product identified by TEM diffraction pattern is Mo_5As_4. (The RHEED pattern is very rich in details, which are more difficult to explain.)

For W grown at $T_s = 300$ °C, the TEM patterns indicate a preferred growth of (111) W parallel to (100) GaAs, but unlike Mo, its [1$\bar{1}$1] direction is rotated by some 13° relative to the GaAs [0$\bar{1}$1] (in the diffraction pattern, the arcs span much larger angles). The (100) W is present to some extent too, but without any epitaxial orientation. For $T_s > 500$ °C, a chemical reaction between the W and the GaAs takes place,

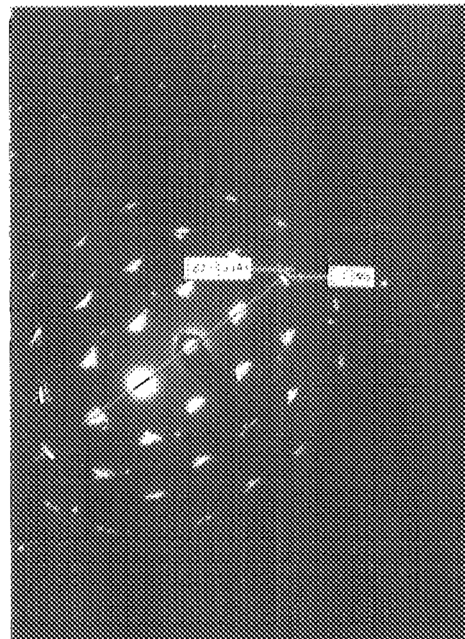

FIG. 3. Electron diffraction pattern of a 150-Å-thick Mo film grown on (100) GaAs at 310 °C. The (100) GaAs which is characterized by dots and the (111) Mo by the short arcs are shown simultaneously in the pattern.

Downloaded 16 Aug 2008 to 132.77.4.43. Redistribution subject to AIP license or copyright; see http://apl.aip.org/apl/copyright.jsp

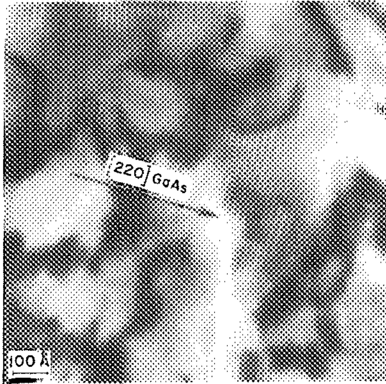

FIG. 4. TEM bright-field of the film described in Fig. 3. Notice the small misorientations between the Moiré fringes of different crystallites in the same domain.

but the reaction products had not been identified.

AES measurements, taken immediately after the deposition, did not detect any As or Ga on 150-Å-thick Mo films grown at T_s up to 200 °C. Thereafter, the surface As content increased up to 25% for 250 °C $< T_s <$ 450 °C. Ga was detected only at $T_s = 400$ °C and increased considerably at higher temperatures. As and Ga were found on W films grown at temperatures as low as room temperature. Since the electron diffraction results do not show any compound formation at temperatures below 500 °C, out-diffusion of As and Ga to the W film surface probably takes place.

Current-voltage (I-V) and capacitance-voltage (C-V) techniques were used to obtain the Mo-GaAs and W-GaAs Schottky barrier heights corresponding to growth at several substrate temperatures. Devices were processed by forming mesa structures (1 mm^2 and 0.25 mm^2) and an alloyed NiAuGe ohmic contact at the back of the n^+-GaAs substrate. Approximately 1000 Å of Mo and W were evaporated on top of the Mo and W thin films, respectively, in order to assist in the top contact formation. Schottky barrier heights (ϕ_b) and ideality factors (n) were calculated[16] from the I-V and C-V results and are listed in Table I.

While ϕ_b^{CV} does not show any trend, ϕ_b^{IV} is increased slightly with growth temperature, which might be related to As out-diffusion. Note that at $T_s = 520$ °C, where the reaction between the Mo and GaAs starts taking place, the ideality factor n is considerably higher, whereas the barrier height is almost unchanged. These results are similar to those previously published[10] and exhibit similar differences between ϕ_B^{IV} and ϕ_B^{CV}. Since the existence of any oxide at the interface is unlikely, the low ϕ_B^{IV} and the high n suggest some additional current transfer mechanisms, which could be related to a nonideal interface; this interface, in turn, might have a different dielectric constant, thus affecting ϕ_B^{CV}.

The obvious differences between the growth of W and Mo could be related to differences in atom mobilities and reactivity with the GaAs substrates. The existence of Ga and As on the surfaces of both suggests that *very clean* W and Mo are not necessarily good diffusion barriers for Ga and As. Moreover, if reactions below our detection sensitivity limits do take place at the interfaces (for $T_s <$ 500 °C), their influences on the Schottky barrier are negligible.

In summary, Mo epitaxial layers were grown on (100)

TABLE I. Schottky barriers and ideality factors of metal-GaAs interfaces for several substrate temperatures.

Metal	T_s (°C)	ϕ_B^{CV} (eV)	Φ_b^{IV} (eV)	n
Mo	100	1.00 ± 0.01	0.70	1.21 ± 0.03
	270	1.03 ± 0.03	0.70	1.18 ± 0.01
	310	1.02 ± 0.03	0.72	1.18 ± 0.02
	370	1.03 ± 0.02	0.73	1.19 ± 0.01
	520	0.97 ± 0.03^b	0.735	1.31 ± 0.08
W	40	0.97 ± 0.03	0.74	1.15 ± 0.01
	300	0.99 ± 0.03	0.72	1.21 ± 0.03

[a] Experimental errors were $< \pm 0.01$ for all I-V measurements. $A^{**} = 8.4$ cm^{-2} K^{-2} was assumed.
[b] $1/C^2$ was not linear for voltage above 1 V. The results were obtained from this range.

GaAs planes at temperatures between 200 and 400 °C. The orientation relation is (111) Mo || (100) GaAs with [0$\bar{1}$1] Mo || [0$\bar{1}$1] GaAs. The films grew in a form of relatively large domains consisting of smaller grains, which were all arranged in the same orientation. At lower temperatures, the Mo films grew in a polycrystalline fashion. Epitaxial W films are not formed under similar experimental conditions. Out-diffusion of As and Ga is evident at relatively low temperatures, but the effect on Schottky barrier characteristics is small. Above $T_s \approx 500$ °C, the metals react with the GaAs (with Mo_4As_5 as the the main products for the Mo-GaAs system).

We would like to thank H. Euler for constructing the e-guns; and D. Guarnieri and J. O'Sullivan for their help in the design and testing of the e-guns. We also thank L. Osterling and D. Thomas for their technical assistance and A. Segmuller for the x-ray data. M. Eizenberg and D. Smith are gratefully acknowledged for their helpful suggestions and for reviewing the manuscript.

[1] J. A. Calviello, J. L. Wallace, and P. R. Bie, IEEE Trans. Electron Devices **ED-21**, 624 (1974); H. R. Fetterman, P. E. Tennenwald, B. J. Clifton, C. D. Parker, and W. D. Fitzgerald, Appl. Phys. Lett. **33**, 151 (1978).
[2] S. M. Sze, *Physics of Semiconductor Devices* (Wiley, New York, 1981), Chaps. 5 and 6.
[3] J. M. Shannon, Solid State Electron Devices **3**, 142 (1979).
[4] N. Braslau, J. Vac. Sci. Technol. B **1**, 700 (1983).
[5] J. M. Woodall and J. L. Freeouf, J. Vac. Sci. Technol. **19**, 794 (1981); S. H. Pan, D. Mo, W. G. Petro, J. Lindau, and W. E. Spicer, J. Vac. Sci. Technol. B **1**, 593 (1983).
[6] A. Y. Cho and P. O. Dernier, J. Appl. Phys. **49**, 3328 (1978).
[7] R. Ludeke, J. Vac. Sci. Technol. B **2**, 400 (1984).
[8] K. Suh, H. K. Park, and K. L. Moazed, J. Vac. Sci. Technol. B **1**, 365 (1983).
[9] A. K. Shina and J. M. Poate, Appl. Phys. Lett. **24**, 666 (1973); J. G. Smith and P. Brook, J. Vac. Sci. Technol. **16**, 138 (1979); S. D. Makherjee, C. J. Palmstron, and J. G. Smith, J. Vac. Sci. Technol. **17**, 904 (1980); P. M. Batev, M. D. Ivanovitch, E. I. Kafedjiiska, and S. S. Simeonov, Int. J. Electron. **48**, 511 (1980).
[10] J. R. Waldrop, S. P. Kowalczyk, and R. W. Grant, J. Vac. Sci. Technol. **21**, 607 (1982), J. R. Waldrop, Appl. Phys. Lett. **41**, 350 (1982).
[11] G. A. Prinz, G. T. Rads. and J. T. Krebs, J. Appl. Phys. **53**, 2087 (1982).
[12] B. A. Unvala, Le Vide **104**, 109 (1963).
[13] *Handbook of Thin Film Technology*, edited by L. I. Maissel and R. Glang (McGraw-Hill, New York, 1970), pp. 1–51.
[14] M. Heiblum, J. Bloch, and J. J. O'Sullivan (unpublished).
[15] M. Heiblum, E. E. Mendez, and L. Osterling, J. Appl. Phys. **54**, 6982 (1983).
[16] S. M. Sze, *Physics of Semiconductors Devices* (Wiley, New York, 1981), Chap. 5.5, pp. 270–297.

Downloaded 16 Aug 2008 to 132.77.4.43. Redistribution subject to AIP license or copyright; see http://apl.aip.org/apl/copyright.jsp